Structural Engineering and Mechanics, *Vol. 74, No. 1 (2020) 91-104*
DOI: https://doi.org/10.12989/sem.2020.74.1.091

Comparative study of torsional wave profiles through stratified media with fluted boundaries

Manisha Maity*, Santimoy Kundu[a], Alka Kumari[b] and Shishir Gupta[c]

Department of Mathematics and Computing, Indian Institute of Technology (Indian School of Mines) Dhanbad, India

(Received March 11, 2019, Revised October 29, 2019, Accepted November 12, 2019)

Abstract. A mathematical analysis has been carried out for understanding the traversal attributes of torsional waves in a Voigt-type viscoelastic porous layer bounded with corrugated surfaces resting over a heterogeneous transversely isotropic gravitating semi-infinite medium. Both the media are assumed to be under the effect of initial stresses acting along horizontal directions. In the presumed geometry, continuous and periodic type of corrugation has been considered. The condensed form of dispersion relation has been obtained analytically with the aid of the Whittaker's function and suitable boundary conditions. The influence of viscoelasticity, porosity, initial stresses, heterogeneity, gravity, undulation and position parameters on the phase and damped velocities has been illustrated graphically. In addition, relative examination investigating the impact of corrugated and planar bounded surfaces on the dispersion and damping characteristics is one of the important highlights of this study.

Keywords: torsional waves; Voigt-type viscoelastic; porous; Whittaker's function; corrugation; phase velocity; damped velocity

1. Introduction

The vast majority of the geographical compositions of the Earth's crust are found to be porous or permeable media saturated with some sort of fluid. The reason behind this phenomenon is that underneath the Earth's surface, permeable materials are available as coal, sandstones, petroleum reservoirs, etc. pervaded by water or oil. Further, some of the media are porous as well as viscoelastic in nature. For example, settlement and the unification of clay in substructures, porous rocks soaked with viscoelastic fluids, creep at elevated temperature in a permeable wall cooling, etc. The analysis of seismic surface waves through different regimes on Earth, comprising of poro-viscoelastic media is one of the major concerns for the researchers and seismologists round the globe. Hence, in the last few decades, the dynamic traits of poro-viscoelastic media have become the cynosure in the field of seismology; civil, geotechnical and earthquake engineering; soil and rock mechanics and many more.

Porous materials consist of solid and pore components. When one or more fluids are filled inside the pores, then the medium is distinguished as fluid saturated porous medium. Since, there are two components of the fluid saturated porous medium, hence there exist two different types of motion for both the components separately. Moreover, the presence of fluid inside the pores remarkably influences the traversal attributes, such as phase and damped velocities of surface waves. A number of articles are available on account of various conceivable applications of traversal of seismic waves through porous media. The speculation regarding the viscoelasticity of a porous anisotropic solid has been developed by Biot (1956a). Winkler and Nur (1979) experimentally verified the dominance of pore fluids not only on seismic wave velocities but also on seismic attenuation. Alam *et al.* (2018) briefly investigated the nature of phase velocity curves of torsional surface waves propagating through an intermediate poroelastic stratum lying between a stratum and a substratum of inhomogeneous as well as sandy type. Further, a comparative analysis has been carried out by Gupta *et al.* (2018) to irradiate the scattering of torsional waves in a layered Earth's model. In their analysis, a fluid saturated porous medium as well as a transversely isotropic medium have been considered for the topmost layer one by one for two different cases.

Viscoelasticity is a special characteristic of materials that display both viscous and elastic behaviors when subjected to distortion. The most determining attribute of the viscoelastic materials is their ability to absorb the high amount of energy produced during earthquakes and volcanic eruptions. Hence, to withstand the tremors during an earthquake, some of the metal alloys possessing viscoelastic property are utilized as dampers in the construction of multi-storey buildings. With the aid of suitable differential equations, Sharma and Gogna (1991) found a general solution irradiating the traversal behavior of seismic surface waves in a viscoelastic porous semi-infinite

*Corresponding author, Ph.D. Student
E-mail: manishamaity2@gmail.com
a Associate Professor
E-mail: kundu_santi@yahoo.co.in
b Ph.D. Student
E-mail: alkaism@outlook.com
c Professor
E-mail: shishir_ism@yahoo.com

ISSN: 1225-4568 (Print), 1598-6217 (Online)

medium. Modelling of seismic waves in viscoelastic media has been accomplished by Carcione (1993). Abo-Dahab *et al.* (2016) examined the impact of viscoelasticity, heterogeneity and reinforcement on the propagation of surface waves in a rotating anisotropic medium of higher order. Moreover, the impact of physical parameters like heterogeneity, dissipation factor, attenuation coefficient, sandiness, initial stress and thickness ratio on the phase and damped velocities of torsional waves in a viscoelastic stratified Earth's structure has been analytically irradiated by Alam *et al.* (2017). The attenuation and dispersion attributes of torsional waves in a pre-stressed viscoelastic layered structure have been elucidated by Maity *et al.* (2018).

Our Earth is a pre-stressed medium. A large quantity of initial stress often gets generated in a medium because of several natural and artificial phenomena such as difference in gravity, temperature, weight, hydrostatic tension or compression, differential external forces, slow process of creep, presence of overburdened layer, manufacturing activities, external loading etc. Initial stresses exhibit prominent impact not only on the traversal characteristics of elastic waves but also on the stability of the medium. Therefore, it is of great area of interest to the scientists and researchers to examine the effect of these stresses on the propagation traits of elastic waves due to their wide range of applications in numerous fields, including geophysics, seismology, mechanics of composites, rock mechanics, bio-mechanics, non-destructive stress analysis, etc. Ozturk and Akbarov (2009) and Romenski *et al.* (2014) illustrated the traversal of surface waves in various pre-stressed elastic media. The traversal attributes, namely, phase and damped velocities of SH-waves in an inhomogeneous viscoelastic layer lying between an anisotropic porous layer and an initially stressed isotropic half-space have been studied graphically by Kundu *et al.* (2017). Alam *et al.* (2018) discussed the impact of a point source at the interface of a hydrostatically stressed magneto-viscoelastic stratum and a fiber-reinforced substratum of inhomogeneous kind on the propagation of Love-type waves. Gupta and Ahmed (2017) elaborated the impact of initial stress on the traversal behavior of Rayleigh waves in an orthotropic layer lying over a transversely isotropic dissipative half-space. Further, the effect of initial stress and inter facial imperfection on the propagation of shear waves through a piezoelectric stratum resting over a micropolar substratum has been investigated by Kumar *et al.* (2019).

A persistent change in the material properties of any medium due to some natural or artificial phenomena is the principal reason behind the generation of heterogeneity in various layered structures of the Earth. In order to study seismic wave propagation, it is very much important to know the distribution of heterogeneity of Earth, both at the micro and mini scale. With the assistance of surface and body waves, tomographic studies are one of the significant tools in congregating knowledge about seismic heterogeneity. The presence of heterogeneity in a particular medium influences the traversal pattern of surface waves to a large extent. Hence, the study of seismic waves in heterogeneous media has attracted several eminent researchers both in the field of theoretical as well applied seismology. Selim (2007) briefly analysed the noteworthy influence of heterogeneity and surface irregularity on the traversal of torsional waves. A mathematical study has been contemplated by Kakar and Kakar (2016) describing the effect of initial stress, heterogeneity, gravity and porosity on the propagation behavior of SH-waves. Furthermore, the impact of exponential type of heterogeneity on the propagation of shear waves in a sandwiched elastic medium having voids has been presented by Gupta *et al.* (2017). Alam *et al.* (2018) considered six materials, namely beryl, magnesium, cadmium, zinc, cobalt and simply isotropic in order to demonstrate the traversal traits of Love-type waves in a magneto-elastic transversely isotropic layer resting over a heterogeneous half-space induced by a point source.

Each and every particle on Earth, whether its size is big or small possesses different kinds of motion (rotational, translational etc.) about its center of gravity. The motion generated due to the gravitational field is one of the significant features of any media and it also generates internal friction, thus rendering a prominent influence on the equations of motion. Hence, in order to analyze various physical and dynamical problems related to the Earth, the consideration of gravity becomes quite inevitable. A few decades ago, De and Sen-Gupta (1974) slightly modified the Biot's theory of initial stress and assumed that the gravitational force engenders a special kind of initial stress of hydrostatic nature. Based on this hypothesis, they made an attempt to study the nature of wave velocity under the effect of gravity. Also, Ahmed (1999) established the determinant form of frequency relation by considering Rayleigh waves traversing through a granular layer resting over a granular half-space under the influence of gravity. The explicit form of the dispersion relations of Stoneley waves propagating in a gravitating elastic medium for different cases has been elaborately discussed by Vinh and Seriani (2010). Alam *et al.* (2018) graphically demonstrated the influence of magneto-elasticity, hydrostatic stress and gravity on the phase velocity of Rayleigh waves propagating in a layered structure possessing sliding contact.

It is notable from the real life scenario that the superficial layers of the Earth are not always smooth or planar, rather they are more undulated or fluted in their actual form. Some of the examples of corrugated or fluted boundaries are mountains, salt and mineral sediments, rooftops, rides in carnivals, etc. These imperfect surfaces or interfaces of various stratified media in the Earth's crust certainly alter the transmission attributes of elastic waves to a great extent. Thus, the study of seismic waves through irregular boundaries has become a matter of interest among several geophysicists and seismologists worldwide. Tomar and Kaur (2007) applied the Rayleigh's method to approximate the reflection and transmission coefficients of SH-waves at a corrugated interface between two dissimilar semi-infinite media. Recently, with the aid of Green's function, the impact of corrugated interfaces on the diffraction of seismic waves in an elastic medium has been demonstrated by Elmorabie and Yahya (2017). Moreover, Alam *et al.* (2018) irradiated the importance of corrugation on the phase velocity of SH-waves traversing through a

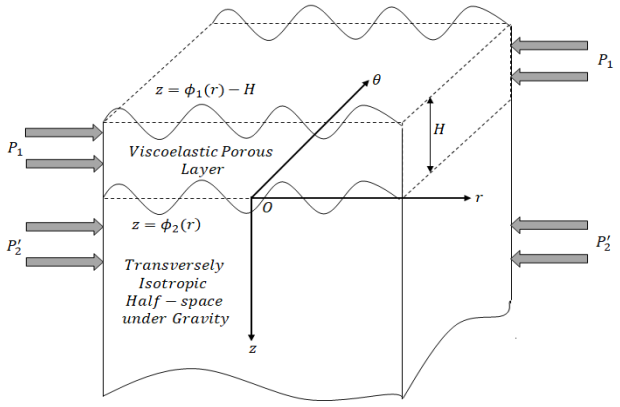

Fig. 1 Structure of the stratified model of the Earth

magneto-elastic anisotropic medium overlying a heterogeneous half-space.

This theoretical analysis unfolds the impact of porosity, viscoelasticity, initial stresses, heterogeneity, gravity and corrugation on the propagation characteristics of torsional surface waves. With the assistance of appropriate equations of motion and variable separable technique, the displacement components corresponding to the layer and half-space have been deduced separately. From the obtained displacement components along with suitable boundary conditions, the condensed form of dispersion equation has been derived. Moreover, due to the consideration of Voigt-type viscoelastic superficial layer as well as a complex form of wave number, the dispersion equation of our presumed geometry gets transformed to its complex form. With the aid of software Mathematica, the complex dispersion equation has been split into real and imaginary components. These real and imaginary components delineate the dispersion and damping phenomena of torsional waves, respectively. Thus, the velocity related with dispersion is termed as phase velocity (V_P) whereas the velocity related with damping is termed as damped velocity (V_D). The influence of corrugation along with different varying magnitudes of other parameters on the phase and damped velocities of torsional waves has been elucidated graphically. Permeable rocks saturated with viscoelastic fluids, stresses in a dam and stream of oil or any kind of fluid in oil supplies are some of the media exhibiting the poro-viscoelastic property. Moreover, the presence of corrugated boundaries can be naturally found in salt and mineral sediments, sand dunes in deserts, mainland edges, mountains, etc. The present investigation may thus find its applications in the study of seismic prospecting techniques in such regions of the Earth's crust.

2. Mathematical formulation of the problem

A Voigt-type viscoelastic porous layer,

$$M_I : \phi_1(r) - H \le z \le \phi_2(r)$$

resting over a heterogeneous transversely isotropic half-space, $M_{II}: \phi_2(r) \le z \le \infty$ has been contemplated in our presumed model. Here, H is the finite width; and $z = \phi_1(r) - H$ and $z = \phi_2(r)$ are the equations of the corrugated top and bottom boundaries of the considered layer. Also, the half-space has been assumed to be under the influence of gravity. A cylindrical coordinate system has been undertaken in which the torsional waves are presumed to traverse along the radial direction (r-axis) with velocity c. Moreover, the directions of z-axis and θ-axis are taken to be vertically downwards and along the horizontal plane of the cylindrical coordinate system, respectively. Both the layer and half-space are under the impact of initial stresses P_1 and P_2' respectively, acting horizontally parallel to r-axis. It has been considered that the initial stress, elastic constants and density of the half-space vary exponentially with depth. The aforesaid geometrical structure of our problem has been depicted in Fig. 1. The Fourier series representation of the continuous and periodic functions $\phi_1(r)$ and $\phi_2(r)$ as established by Asano (1966) may be written as:

$$\phi_n(r) = \sum_{m=1}^{\infty}\left(\phi_m^n e^{im\beta r} + \phi_{-m}^n e^{-im\beta r}\right); \quad n = 1,2, \tag{1}$$

where ϕ_m^n and ϕ_{-m}^n are the coefficients and m is the order of the Fourier series expansion. Moreover, the constant entities γ_n, S_m^n and T_m^n may be defined as

$\phi_{\pm 1}^n = \frac{\gamma_n}{2}$ and $\phi_{\pm m}^n = \frac{(S_m^n \mp i T_m^n)}{2}$; $n = 1,2$ and $m = 2,3,\ldots$
Hence, Eq. (1) can be written as

$$\phi_n(r) = \gamma_n \cos(\beta r) + \sum_{m=2}^{\infty}\begin{pmatrix} S_m^n \cos(m\beta r) \\ +T_m^n \sin(m\beta r)\end{pmatrix}; \quad n = 1,2. \tag{2}$$

In our present work, the expansion of the series represented in Eq. (2) has been considered up to first order. Therefore, the corrugated top and bottom boundaries may be condensed up to only one cosine term i.e., $\phi_n(r) = \gamma_n cos(\beta r), n = 1,2$, where γ_n are the magnitudes of the respective corrugated boundary surfaces and $2\pi/\beta$ is the corrugation wavelength.

3. Fundamental equations and solution

3.1 Dynamics of the viscoelastic porous layer

As per the considered geometry of our problem, let (u_1,v_1,w_1) and (U_1,V_1,W_1) be the displacement of the solid and the liquid constituents of the anisotropic porous layer in the radial (r), azimuthal (θ) and axial (z) directions, respectively. The traversal of torsional surface waves in the layer is distinguished by the following displacement and non-zero strain components:

$$\begin{aligned} &u_1 = u_r^{(1)} = 0,\ v_1 = u_\theta^{(1)} = v_1(r,z,t),\ w_1 = u_z^{(1)} = 0, \\ &U_1 = U_r = 0,\ V_1 = U_\theta = V_1(r,z,t),\ W_1 = U_z = 0, \\ &e_{r\theta}^{(1)} = \frac{1}{2}\left(\frac{\partial v_1}{\partial r} - \frac{v_1}{r}\right) \text{ and } e_{\theta z}^{(1)} = \frac{1}{2}\frac{\partial v_1}{\partial z}. \end{aligned} \tag{3}$$

With the aid *of* relations in (3), the non-zero stress components for the anisotropic Voigt-type viscoelastic

porous layer is given by:

$$\tau_{r\theta}^{(1)} = D_{\mu_N}\left(\frac{\partial v_1}{\partial r} - \frac{v_1}{r}\right) \text{ and } \tau_{\theta z}^{(1)} = D_{\mu_G}\frac{\partial v_1}{\partial z}, \quad (4)$$

where D_{μ_N} and D_{μ_G} are the anisotropic Voigt-type viscoelastic parameters defined as

$$D_{\mu_N} = \mu_N + \mu_N^{'}\frac{\partial}{\partial t} \text{ and } D_{\mu_G} = \mu_G + \mu_G^{'}\frac{\partial}{\partial t},$$

where μ_N and μ_G are the shear moduli along longitudinal and transverse directions, respectively. Also, μ_N' and μ_G' are the internal frictions along the longitudinal and transverse directions, respectively.

The governing pair of equation of motion for the traversal of torsional waves through a pre-stressed viscoelastic porous layer in the absence of body force given by Biot (1965) is written as

$$\begin{aligned}&\frac{\partial}{\partial r}\tau_{r\theta}^{(1)} + \frac{\partial}{\partial z}\tau_{\theta z}^{(1)} + \frac{2}{r}\tau_{r\theta}^{(1)}\\ &-P_1\frac{\partial}{\partial r}\omega_z^{(1)} = \frac{\partial^2}{\partial t^2}\left(\rho_{rr}^{(1)}v_1 + \rho_{r\theta}^{(1)}V_1\right)\end{aligned} \quad (5)$$

$$\text{and} \quad \frac{\partial^2}{\partial t^2}\left(\rho_{r\theta}^{(1)}v_1 + \rho_{\theta\theta}^{(1)}V_1\right) = 0, \quad (6)$$

where $\omega_z^{(1)} = \frac{1}{2r}\left(\frac{\partial(rv_1)}{\partial r} - \frac{\partial v_1}{\partial \theta}\right)$ is the axial rotational component. Also, $\rho_{rr}^{(1)}$, $\rho_{\theta\theta}^{(1)}$ and $\rho_{r\theta}^{(1)}$ are the coefficients of mass obeying the following inequalities:

$$\rho_{rr}^{(1)} > 0,\ \rho_{\theta\theta}^{(1)} > 0,\ \rho_{r\theta}^{(1)} < 0 \text{ and } \rho_{rr}^{(1)}\rho_{\theta\theta}^{(1)} - (\rho_{r\theta}^{(1)})^2 > 0.$$

It is considered that there does not exist any kind of correlative movement between the liquid and solid components of the porous medium. Hence, $\rho_{rr}^{(1)}$, $\rho_{\theta\theta}^{(1)}$ and $\rho_{r\theta}^{(1)}$ are associated with the overall density (ρ_1) of the porous layer and densities of solid phase ($\rho_s^{(1)}$) and liquid phase ($\rho_w^{(1)}$), by the following relations given by Biot (1956b, c):

$$\begin{aligned}&\rho_{rr}^{(1)} + \rho_{r\theta}^{(1)} = (1-f_p)\rho_s^{(1)}\\ &\text{and } \rho_{r\theta}^{(1)} + \rho_{\theta\theta}^{(1)} = f_p\rho_w^{(1)},\end{aligned} \quad (7)$$

where the layer's porosity is denoted by f_p. Thus, with the help of Eq. (7), the density of the layer is given by

$$\rho_1 = \rho_{rr}^{(1)} + 2\rho_{r\theta}^{(1)} + \rho_{\theta\theta}^{(1)} = \rho_s^{(1)} + f_p(\rho_w^{(1)} - \rho_s^{(1)}). \quad (8)$$

Applying Eqs. (4) and (6), Eq. (5) gets converted to

$$\left(D_{\mu_N} - \frac{P_1}{2}\right)\left(\frac{\partial^2 v_1}{\partial r^2} + \frac{1}{r}\frac{\partial v_1}{\partial r} - \frac{v_1}{r^2}\right) + D_{\mu_G}\frac{\partial^2 v_1}{\partial z^2} = d_1^{'}\frac{\partial^2 v_1}{\partial t^2}, \quad (9)$$

where d_1' is defined in Appendix-I.

For a harmonic wave propagating along r-axis, the solution of Eq. (9) may be considered of the form as

$$v_1(r,z,t) = V(z)J_1(kr)e^{i\omega t}, \quad (10)$$

where k =wave number, ω(=kc) =angular frequency, c =torsional wave velocity and $J_1(kr)$ = Bessel's function of first kind and first order.

Substituting Eq. (10) into Eq. (9), we obtain

$$\frac{d^2V(z)}{dz^2} + k^2\xi^2V(z) = 0, \quad (11)$$

where ξ is defined in Appendix-I.

The solution of (11) is procured as

$$V(z) = M_1\cos(k\xi z) + M_2\sin(k\xi z), \quad (12)$$

where M_1 and M_2 are constants.

Hence, the desired displacement component of torsional surface waves in the considered layer is written as

$$v_1(r,z,t) = \left(M_1\cos(k\xi z) + M_2\sin(k\xi z)\right)J_1(kr)e^{i\omega t}. \quad (13)$$

3.2 Dynamics of the transversely isotropic half-space

For the propagation of torsional surface waves, let (u_2, v_2, w_2) be the displacement components of the half-space obeying the following condition

$$\begin{aligned}&u_2 = u_r^{(2)} = 0, \quad v_2 = u_\theta^{(2)}\\ &= v_2(r,z,t) \text{ and } w_2 = u_z^{(2)} = 0.\end{aligned} \quad (14)$$

Further, let us consider that the initial stress (P_2'), elastic constants ($\mu_{11}^{'}, \mu_{12}^{'}$ and $\mu_{44}^{'}$) and density (ρ_2') of the half-space vary exponentially with depth, i.e.,

$$\begin{aligned}&P_2^{'}(z) = P_2e^{qz},\ \mu_{11}^{'}(z) = \mu_{11}e^{qz},\ \mu_{12}^{'}(z) = \mu_{12}e^{qz},\\ &\mu_{44}^{'}(z) = \mu_{44}e^{qz} \text{ and } \rho_2^{'}(z) = \rho_2e^{qz},\end{aligned} \quad (15)$$

where q is the heterogeneity of the half-space having dimension same as that of inverse of length.

In the absence of body forces, the only non-vanishing equation of motion for the transversely isotropic half-space under initial stress and gravity as given by Biot (1965) is written as

$$\begin{aligned}&\frac{\partial\tau_{r\theta}^{(2)}}{\partial r} + \frac{\partial\tau_{\theta z}^{(2)}}{\partial z} + \frac{2\tau_{r\theta}^{(2)}}{r} + \frac{\partial}{\partial z}\left[\left(P_2^{'}(z) - \rho_2^{'}(z)gz\right)e_{\theta z}^{(2)}\right]\\ &\quad - \rho_2^{'}(z)gz\frac{\partial}{\partial r}\left[\frac{1}{2}\left(\frac{\partial v_2}{\partial r} + \frac{v_2}{r}\right)\right] = \rho_2^{'}(z)\frac{\partial^2 v_2}{\partial t^2},\end{aligned} \quad (16)$$

where g is the acceleration due to gravity.

For the half-space under the influence of initial stress and gravity, the stress- strain relations are given by

$$\tau_{r\theta}^{(2)} = \left(\mu_{11}^{'}(z) - \mu_{12}^{'}(z)\right)e_{r\theta}^{(2)} \text{ and } \tau_{\theta z}^{(2)} = 2\mu_{44}^{'}(z)e_{\theta z}^{(2)}, \quad (17)$$

where $\tau_{r\theta}^{(2)}$ and $\tau_{\theta z}^{(2)}$ are the stress components; and $e_{r\theta}^{(2)}$ and $e_{\theta z}^{(2)}$ are the strain components defined by

$$e_{r\theta}^{(2)} = \frac{1}{2}\left(\frac{\partial v_2}{\partial r} - \frac{v_2}{r}\right) \text{ and } e_{\theta z}^{(2)} = \frac{1}{2}\frac{\partial v_2}{\partial z}. \tag{18}$$

Using the relations (15), (17) and (18), Eq. (16) becomes

$$\begin{aligned}\frac{1}{2}((\mu_{11}-\mu_{12})-\rho_2 gz)\left(\frac{\partial^2 v_2}{\partial r^2}-\frac{v_2}{r^2}+\frac{1}{r}\frac{\partial v_2}{\partial r}\right)+\left(\mu_{44}+\frac{(P_2-\rho_2 gz)}{2}\right)\frac{\partial^2 v_2}{\partial z^2}\\ +\left(q\mu_{44}+\frac{q(P_2-\rho_2 gz)-\rho_2 g}{2}\right)\frac{\partial v_2}{\partial z}=\rho_2\frac{\partial^2 v_2}{\partial t^2}.\end{aligned} \tag{19}$$

For the propagation of a harmonic wave along the radial (r) direction, the solution of (19) can be written as

$$v_2(r,z,t) = V_2(z)\,J_1(kr)e^{i\omega t}, \tag{20}$$

where $V_2(z)$ is the solution of the following second order differential equation,

$$\begin{aligned}&\frac{d^2V_2(z)}{dz^2}+\left(q-\frac{kG^*}{2\left(1+\frac{P_2}{2\mu_{44}}-\frac{G^*zk}{2}\right)}\right)\frac{dV_2(z)}{dz}\\ &-\frac{k^2\left(\frac{\mu_{11}-\mu_{12}}{2\mu_{44}}-\frac{G^*zk}{2}\right)}{\left(1+\frac{P_2}{2\mu_{44}}-\frac{G^*zk}{2}\right)}\left(1-\frac{c^2}{c_2^2\left(\frac{\mu_{11}-\mu_{12}}{2\mu_{44}}-\frac{G^*zk}{2}\right)}\right)V_2(z)=0,\end{aligned} \tag{21}$$

where,G^* and c_2 are defined in Appendix-I.

Substituting,

$$V_2(z) = \psi(z)e^{-\frac{qz}{2}}\left(1+\frac{P_2}{2\mu_{44}}-\frac{G^*zk}{2}\right)^{-\frac{1}{2}}$$

in Eq. (21), we obtain

$$\frac{d^2\psi(z)}{dz^2}+\kappa(z)\psi(z)=0, \tag{22}$$

where $\kappa(z)$ is defined in Appendix-I.

Again, putting $\delta_1 = \frac{4}{G^*}\left(1+\frac{P_2}{2\mu_{44}}-\frac{G^*zk}{2}\right)$ in Eq. (22), we have

$$\frac{d^2\psi(\delta_1)}{d\delta_1^2}+\left(-\frac{1}{4}+\frac{m}{\delta_1}+\frac{1}{4\delta_1^2}-\frac{q^2}{16k^2}\right)\psi(\delta_1)=0, \tag{23}$$

where m is defined in Appendix-I.

Eq. (23) is the the well known Whittaker's equation (Whittaker and Watson (1991)) having solution given by

$$\psi(\delta_1) = N_1 W_{\frac{m}{k_3},0}(k_3\delta_1) + N_2 W_{-\frac{m}{k_3},0}(-k_3\delta_1), \tag{24}$$

where N_1, N_2 are arbitrary constants, $W_{\frac{m}{k_3},0}(k_3\delta_1)$ is the Whittaker's function and k_3 is defined in Appendix-I.

Since, we are concerned with the propagation of torsional surface waves in the half-space, the solution disappears at z→∞ (i.e., at $\delta_1 \to -\infty$) and hence, the solution can be obtained as

$$\psi(\delta_1) = N_2 W_{-\frac{m}{k_3},0}(-k_3\delta_1). \tag{25}$$

Thus, the desired solution of the half-space taken into consideration is obtained as

$$v_2(r,z,t) = \frac{N_2 W_{-\frac{m}{k_3},0}\left(-k_3\frac{4}{G^*}\left(1+\frac{P_2}{2\mu_{44}}-\frac{G^*zk}{2}\right)\right)e^{\frac{-qz}{2}}J_1(kr)e^{i\omega t}}{\left(1+\frac{P_2}{2\mu_{44}}-\frac{G^*zk}{2}\right)^{\frac{1}{2}}}. \tag{26}$$

4. Boundary conditions and dispersion relation

Continuity of displacement and shearing stress components at the common corrugated interface of the layer and half-space; and the stress free case at the upper corrugated surface of the layer provide suitable boundary conditions, mathematically manifested as:

(1) At the common corrugated interface $z = \phi_2(r)$, the displacement components are continuous,

$$i.e.,\ v_1 = v_2$$

(2) Again at the common corrugated interface $z = \phi_2(r)$, the shearing components of stresses are continuous,

$$i.e.,\ \tau_{\theta z}^{(1)} - \phi_2'(r)\tau_{r\theta}^{(1)} = \tau_{\theta z}^{(2)} - \phi_2'(r)\tau_{r\theta}^{(2)}$$

(3) At the upper corrugated boundary plane(free surface) $z = \phi_1(r) - H$, the shearing stress component vanishes,

$$i.e.,\ \tau_{\theta z}^{(1)} - \phi_1'(r)\tau_{r\theta}^{(1)} = 0$$

Now, using the above three boundary conditions and Eqs. (13) and (26) simultaneously, we obtain the following set of equations:

$$a_{11}M_1 + a_{12}M_2 + a_{13}N_2 = 0, \tag{27}$$

$$a_{21}M_1 + a_{22}M_2 + a_{23}N_2 = 0 \tag{28}$$

$$\text{and } a_{31}M_1 + a_{32}M_2 = 0, \tag{29}$$

where the coefficients a_{11} to a_{13}, a_{21} to a_{23}, a_{31} and a_{32} are well defined in Appendix-I.

Eliminating M_1, M_2 and N_2 from Eqs. (27) to (29), we get

$$\Delta(k,c) = \tan(k\xi(H-\phi_1(r)+\phi_2(r))) - \frac{\chi_1}{\chi_2} = 0, \tag{30}$$

where $\chi_1$and χ_2 are defined in Appendix-II.

Eq. (30) is the desired dispersion equation for the propagation of torsional waves through a corrugated pre-stressed Voigt-type viscoelastic porous layer overlying a pre-stressed heterogeneous transversely isotropic half-space under the influence of gravity.

5. Particular cases

5.1 Case-I

Considering both the top and bottom boundaries of the viscoelastic porous layer to be corrugated i.e., $z = \gamma_1 cos(\beta r) - H$ and $z = \gamma_2 cos(\beta r)$, the dispersion Eq. (30) gets converted to

$$\tan\left(k\xi(H-\gamma_1\cos(\beta r)+\gamma_2\cos(\beta r))\right)=\frac{\chi_{11}}{\chi_{22}}, \quad (31)$$

where χ_{11} and χ_{22} are defined in Appendix-II.

Eq. (31) is the desired dispersion equation for the propagation of torsional waves through a pre-stressed Voigt-type viscoelastic porous layer bounded by upper and lower periodically corrugated boundary surfaces resting over a pre-stressed heterogeneous transversely isotropic half-space under the influence of gravity.

5.2 Case-II

Considering both the top and bottom boundaries of the viscoelastic porous layer to be non-corrugated i.e., $z = -H$ and $z = 0$, the dispersion Eq. (30) gets converted to

$$\tan(k\xi H)=\frac{\mu_{44}(bk_3q\psi_1+\psi_{333})}{2A_{22}bk_3\psi_1}, \quad (32)$$

where ψ_{333} is defined in Appendix-II.

Eq. (32) is the desired dispersion equation for the propagation of torsional waves through a pre-stressed Voigt-type viscoelastic porous layer bounded by upper and lower flat surfaces resting over a pre-stressed heterogeneous transversely isotropic half-space under the influence of gravity.

5.3 Case-III

Considering the layer to be isotropic without initial stress and corrugated boundary surfaces; and the half-space to be isotropic in the absence of heterogeneity, initial stress and gravity, i.e.,

$$\mu_N^{'}=\mu_G^{'}=0,\ \mu_N=\mu_G=\mu_1,\ d_1^{'}/\rho_1\to 1,\ P_1=0,$$

$$\phi_1(r)=\phi_2(r)=0,\ \frac{\mu_{11}-\mu_{12}}{2}=\mu_{44}=\mu_2,\ q=0,$$

$$P_2=0 \text{ and } G^*=0,$$

the dispersion relation (30) gets reduced to

$$\tan(kH\sqrt{\frac{c^2}{c_{11}^2}-1})=\frac{\mu_2\sqrt{1-\frac{c^2}{c_2^2}}}{\mu_1\sqrt{\frac{c^2}{c_{11}^2}-1}}, \quad (33)$$

where c_{11} is defined in Appendix-II.

Eq. (33) coincides with the well established classical equation of Love waves (Love (1920)), thus validating our considered problem.

6. Numerical results and discussion

With the aid of dispersion Eq. (30), a considerable amount of analysis has been carried out to shed light on the traversal characteristics of torsional surface waves through a corrugated pre-stressed Voigt-type viscoelastic porous layer resting over a pre-stressed heterogeneous transversely isotropic half-space under the influence of gravity. In our work, the wave number k has been assumed to be complex, and hence represented as $k = k_1 + ik_2 = k_1(1 + i\delta)$, where k_1 and k_2 are real entities and $\delta = \frac{\mathrm{Im}[k]}{\mathrm{Re}[k]} = \frac{k_2}{k_1} (<< 1)$ is the attenuation coefficient. With the help of the software Mathematica, the dispersion relation (30) has been split into real and imaginary parts elucidated by the following relations,

$$\mathrm{Re}[\Delta(k_1,c,\delta)]=0 \quad (34)$$

$$\text{and } \mathrm{Im}[\Delta(k_1,c,\delta)]=0. \quad (35)$$

Eqs. (34) and (35) generate the phase and damped velocity curves i.e., "V_P versus k_1H" and "V_D versus k_1H", respectively.

The parameters influencing the propagation behavior of torsional waves in our work are

$$\text{porosity } (d_1=d_1^{'}/\rho_1),\ \text{viscoelasticity } (f=\omega\mu_N^{'}/\mu_N,\ f_1=\omega\mu_G^{'}/\mu_G),$$

$$\text{initial stresses } (\zeta_1=\frac{P_1}{2\mu_N}(\text{layer}),\zeta_2=\frac{P_2}{2\mu_{44}}(\text{half}-\text{space})),$$

$$\text{heterogeneity } (q/k_1) \text{ and Biot's gravity } (G=g\rho_2/\mu_{44}k_1).$$

The dominance of these parameters on the phase and damped velocities has been depicted in Figs. 2 to 7 for both the corrugated and planar (non-corrugated) boundary surfaces of the layer. Also, the impact of position (r/H) and undulation (βH) parameters on the traversal of torsional waves has been elucidated in Fig. 8.

The traversal of seismic waves through different kinds of porous media has always been an interesting topic for the researchers and seismologists round the globe. Hence, the points mentioned below are quite notable for understanding the presence of porosity in the layer:

- when the layer is assumed to be a non-porous medium, we get $d_1 \to 1$.
- when the layer is assumed to be a medium containing fluid, we get $d_1 \to 0$.
- when the layer is assumed to be a porous medium, we get $0 < d_1 < 1$.

For plotting of graphs, the following data have been taken into account:

(a) For the corrugated viscoelastic porous layer (Chattaraj and Samal (2013)):

$$\mu_N = 0.2774\times10^{10}\mathrm{N/m^2},\ \mu_G = 0.1387\times10^{10}\mathrm{N/m^2},$$

$$\rho_{rr}^{(1)} = 1.926137\times10^3\mathrm{kg/m^3}, \rho_{r\theta}^{(1)} = -0.002137\times 10^3\mathrm{kg/m^3} \text{and } \rho_{\theta\theta}^{(1)} = 0.215337\times10^3\mathrm{kg/m^3}$$

(b) For the heterogeneous transversely isotropic half-space (Prosser and Green Jr (1990)):

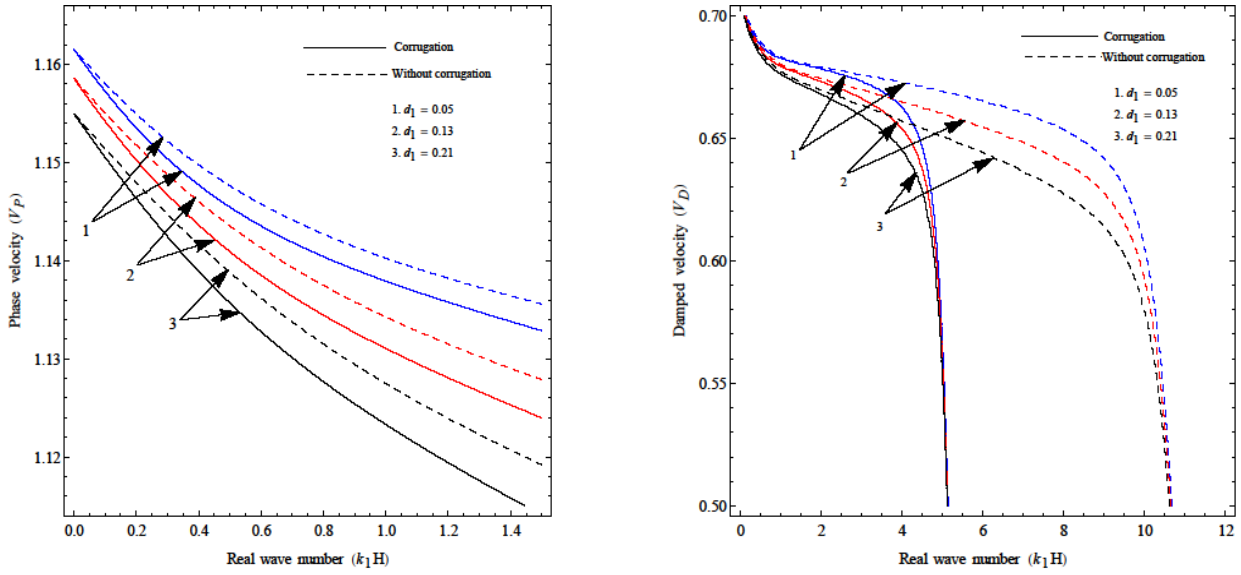

(a) (b)

Fig. 2 Plots of dimensionless (a) phase (V_P) and (b) damped (V_D) velocities as a function of dimensionless real wave number (k_1H) for different magnitudes of porosity parameter (d_1)

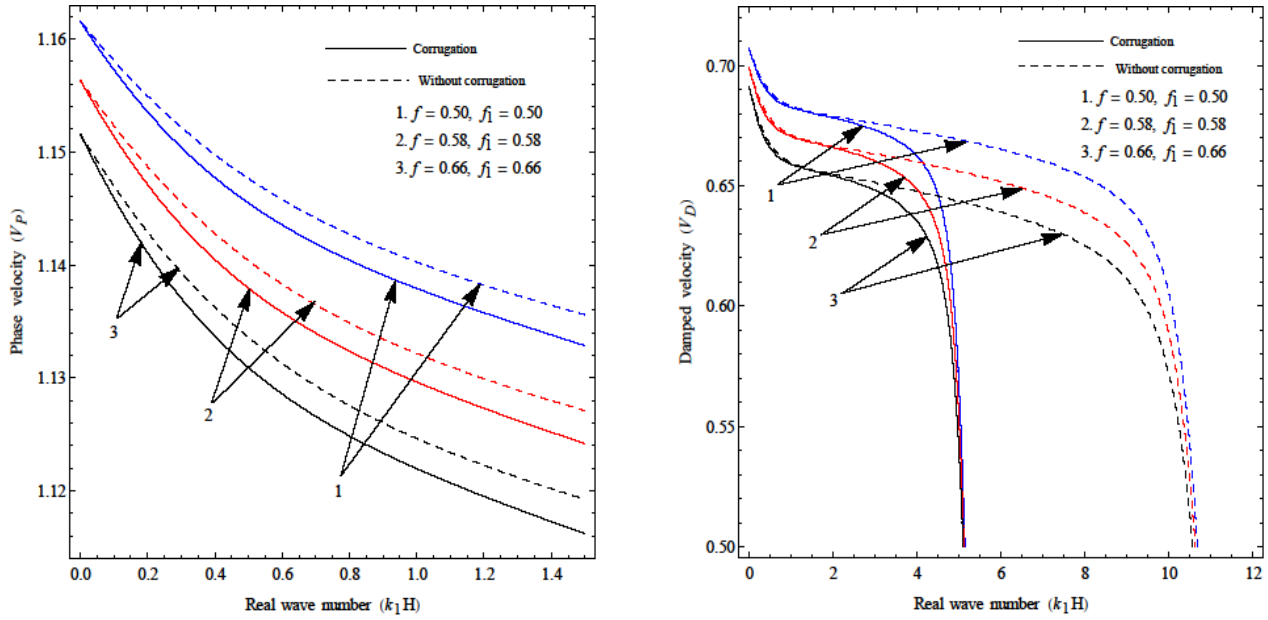

(a) (b)

Fig. 3 Plots of dimensionless (a) phase (V_P) and (b) damped (V_D) velocities as a function of dimensionless real wave number (k_1H) for different magnitudes of viscoelastic parameters (f, f_1)

$\mu_{11} = 1.426\times10^{10}$ N/m^2, $\mu_{12} = 0.678\times10^{10}$ N/m^2, $\mu_{44} = 0.527\times10^{10}$ N/m^2 and $\rho_2 = 1.422\times10^{3}$ kg/m^3.

6.1 Influence of porosity parameter

Figs. 2(a) and 2(b) exemplify the influence of porosity parameter (d_1) associated with the layer on the phase and damped velocity curves i.e., "V_P versus k_1H" and "V_D versus k_1H", respectively. The curves 1, 2 and 3 have been drawn for d_1=0.05, 0.13 and 0.21, respectively. Also, in both the figures a comparative analysis has been carried out to study the propagation characteristics of torsional waves for both corrugation and corrugation free cases.

It is evident from Fig. 2(a) that rising magnitude of porosity disfavors the growth of phase velocity for both the corrugated and planar boundary surfaces of the layer. But for a particular value of porosity parameter the phase velocity in case of planar boundaries is always higher than the phase velocity in case of corrugated boundaries of the layer. Also, the dominance of the porosity parameter on the phase velocity curves can be seen prominently for higher values of wave number.

On the other hand, Fig. 2(b) irradiates the fact that in the presence and absence of corrugation, the damped velocity diminishes with the increasing value of d_1. In both the cases, the damping curves are convergent for lower and

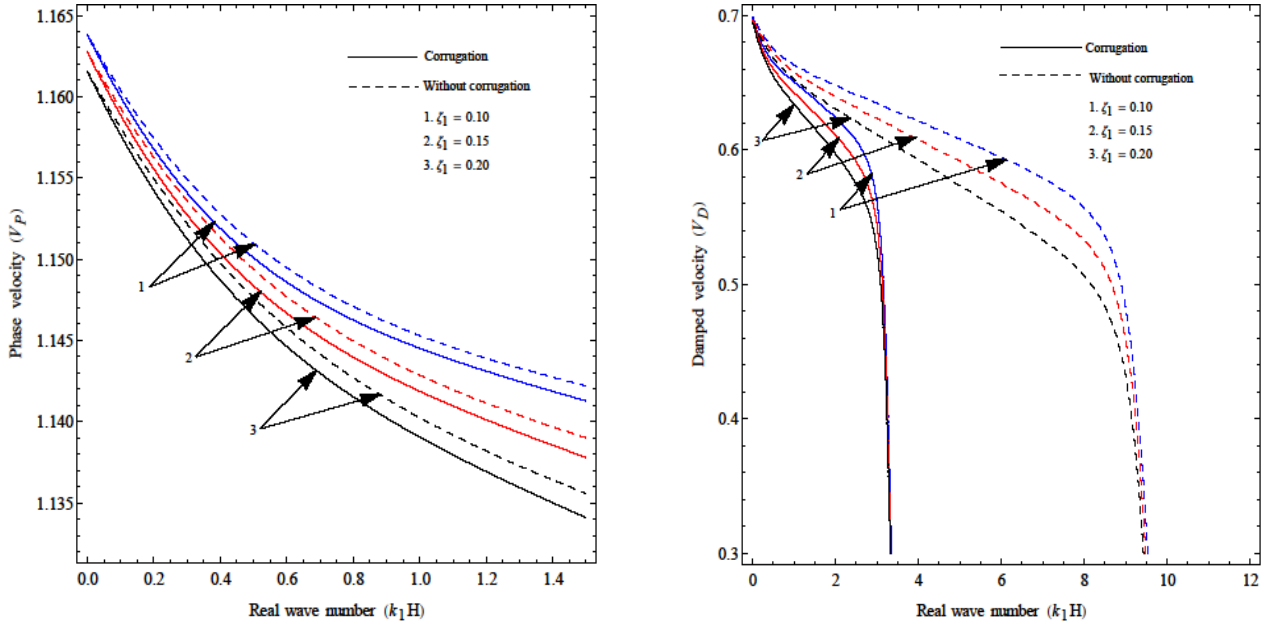

(a) (b)

Fig. 4 Plots of dimensionless (a) phase (V_P) and (b) damped (V_D) velocities as a function of dimensionless real wave number (k_1H) for different magnitudes of initial stress parameter (ς_1)

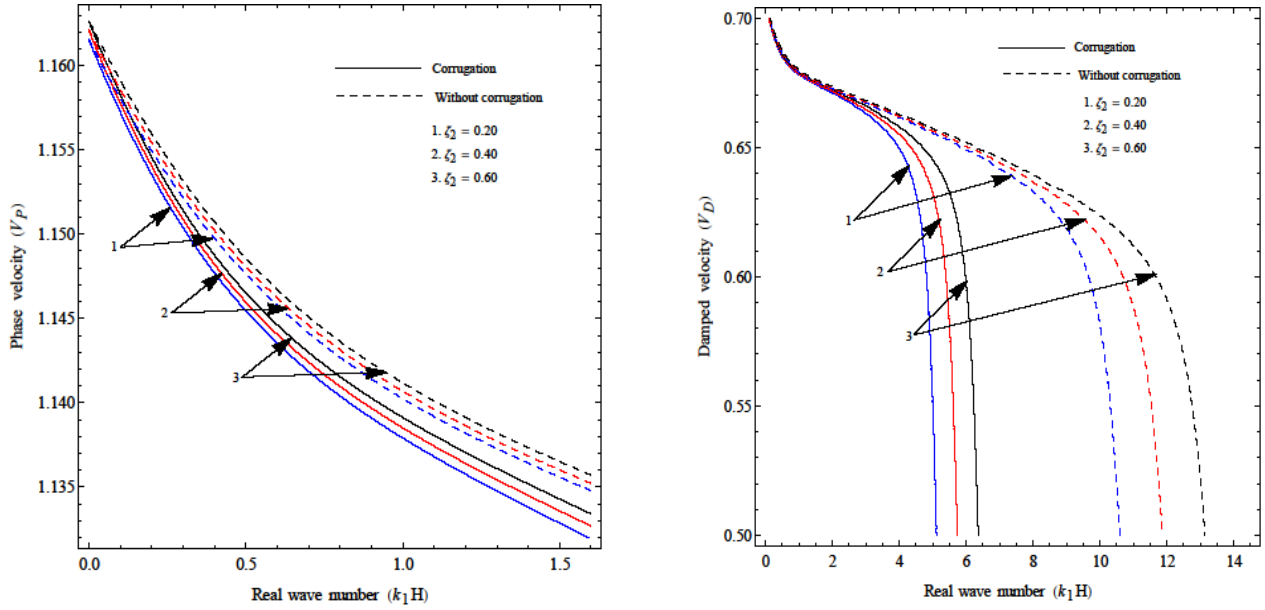

(a) (b)

Fig. 5 Plots of dimensionless (a) phase (V_P) and (b) damped (V_D) velocities as a function of dimensionless real wave number (k_1H) for different magnitudes of initial stress parameter (ς_2)

higher frequencies of wave number which means the impact of d_1 is negligible on the damped velocity at these frequencies of wave number. In addition to this, with the growing value of k_1H, the damped velocity curves fall off quickly in case of corrugated boundaries than in case of planar boundaries.

6.2 Influence of viscoelastic parameters

Figs. 3(a) and 3(b) unravel the behavior of viscoelastic parameters (f, f_1) on the phase and damped velocities of torsional waves by taking parametric values of (f, f_1) as (0.50, 0.50), (0.58, 0.58) and (0.66, 0.66) for curves 1, 2 and 3, respectively. In case of corrugated as well as planar bounded surfaces of the upper medium, it is perceived from

Fig. 3(a) that as the viscoelasticity related with the layer increases, the phase velocity curve shifts downwards.

Moreover, the presence of viscoelasticity is very much effective on the phase velocity for the entire frequency regime of wave number, i.e., in the overall range of wave number, the diminishing behavior of phase velocity of torsional waves is very much noteworthy by considering different values of viscoelastic parameters.

Fig. 3(b) irradiates the damping characteristics of torsional waves for different magnitudes of (f, f_1). Further, the presence of corrugation in the boundary surfaces of the

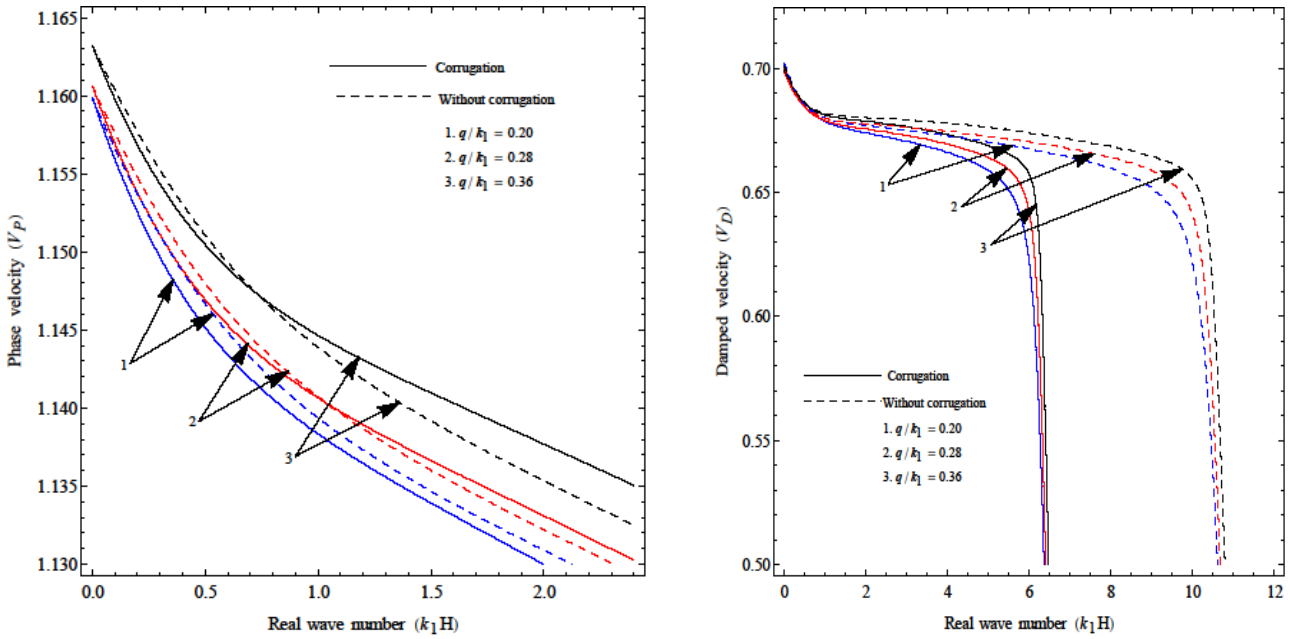

(a) (b)

Fig. 6 Plots of dimensionless (a) phase(V_P) and (b) damped (V_D) velocities as a function of dimensionless real wave number(k_1H) for different magnitudes of heterogeneity parameter (q/k_1)

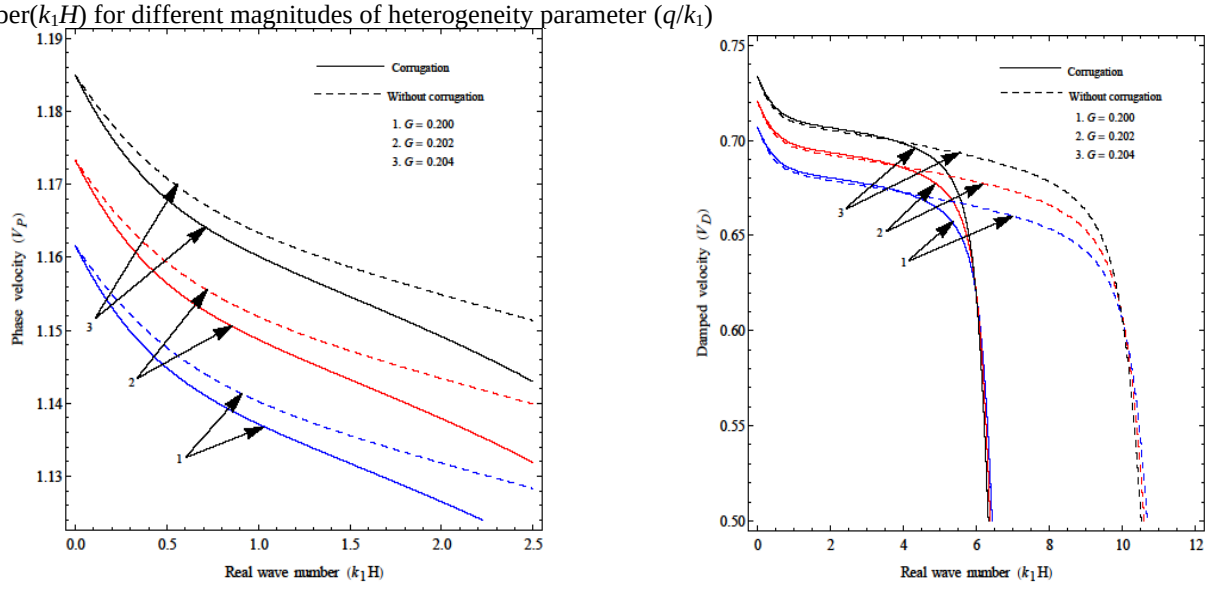

(a) (b)

Fig. 7 Plots of dimensionless (a) phase (V_P) and (b) damped (V_D) velocities as a function of dimensionless real wave number (k_1H) for different magnitudes of gravity parameter (G)

layer is very much vital in determining the attributes related to the damping curves. Initially, for lower values of wave number i.e., $k_1H \leq 2$ and for a fixed magnitude of (f, f_1), the curves corresponding to corrugation and corrugation free cases share a common damped velocity profile. Thus, it can be concluded that the damped velocity of torsional waves is independent of corrugated boundaries of the layer for $k_1H \leq 2$. Contrary to this, the impact of the corrugation is distinguishable for different magnitudes of viscoelasticity and higher values of wave number i.e., $k_1H > 2$. Moreover, irrespective of corrugated boundary surfaces, it is observed that the damped velocity curves 1, 2 and 3 decline with the increasing value of viscoelasticity and wave number.

6.3 Influence of initial stress parameters

The potential dominance of initial stress parameters, i.e., ζ_1 (layer) and ζ_2 (half-space) on traversal characteristics of torsional waves has been delineated through Figs. 4(a) and 4(b); and 5(a) and 5(b), respectively. In addition to initial stresses, the impact of corrugation has also been exhibited graphically through these figures. To examine the effect, the numerical values assigned to ζ_1 and ζ_2 for curves 1, 2 and 3 are 0.10, 0.15 and 0.20; and 0.20, 0.40 and 0.60, respectively.

It is remarked from Figs. 4(a) and 4(b) that escalating value of ζ_1 reduces the growth of both phase and damped velocities. This decreasing trend of phase and damped

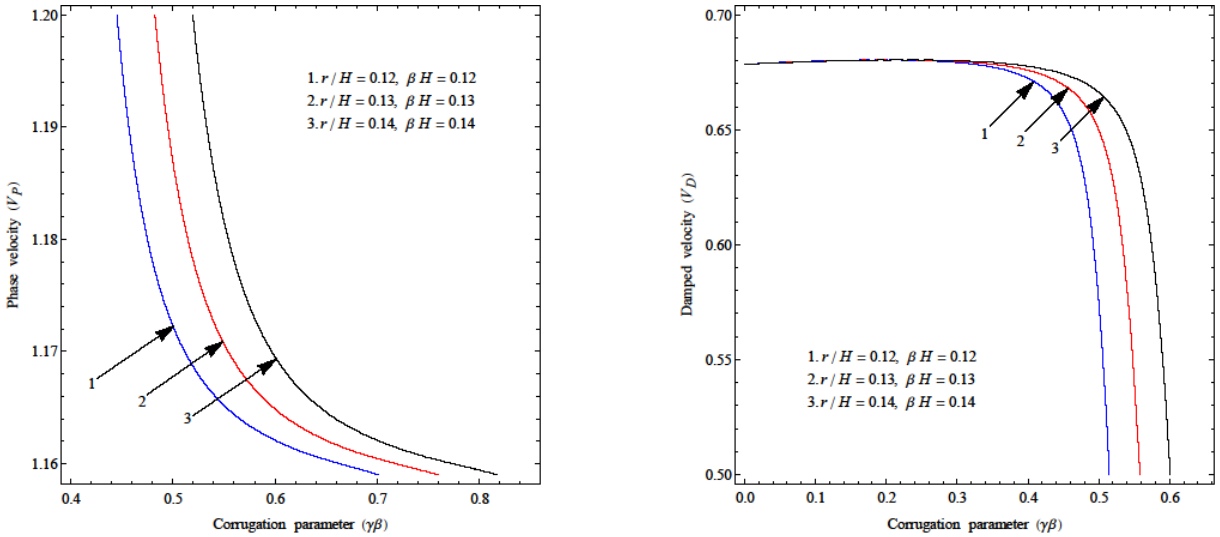

(a) (b)

Fig. 8 Plots of dimensionless (a) phase (V_P) and (b) damped (V_D) velocities as a function of dimensionless real wave number (k_1H) for different magnitudes of position (r/H) and undulatory (βH) parameters

velocity curves is notable for both corrugation and corrugation free cases. Moreover, it is clear from Fig. 4(b) that the damped velocity curves tend to get united in the neighbourhood of k_1H =0, elucidating the fact that in this particular region of wave number, the damping characteristics are independent of the presence of initial stress and undulated boundaries of the layer.

However, Figs. 5(a) and 5(b) irradiate the favourable influence of initial stress parameter of the half-space on the phase and damped velocity curves i.e., both the velocities increase as ζ_2 increases. The impact of ζ_2 is more prominent on damped velocity as compared to phase velocity of torsional waves. Further, emphasising on the effect of corrugation, it can be seen from Fig. 5(a) that the phase velocity curves 1, 2 and 3 related to the corrugated boundary surfaces lie below the phase velocity curves 1, 2 and 3 related to the planar boundary surfaces. Hence, it can be concluded that any medium bounded by corrugated surfaces decreases the phase velocity of torsional waves. Also, it is remarked from Fig. 5(b) that the influence of varying magnitude of ζ_2 on damped velocity curves is more notable in case of planar boundaries rather than corrugated boundaries.

6.4 Influence of heterogeneity parameter

The propagation behavior of torsional waves through our presumed heterogeneous medium has been elucidated through Figs. 6(a) and 6(b). For plotting the phase and damped velocity curves 1, 2 and 3, the magnitudes of the heterogeneity parameter q/k_1 have been taken as 0.20, 0.28and 0.36, respectively.

It is noteworthy from Fig. 6(a) that with the increasing magnitude of heterogeneity in the half-space, the propagation of torsional waves becomes faster for both corrugation and corrugation free cases. Unlike earlier figures, it is observed from Fig. 6(a) that the phase velocity curves 2 and 3 corresponding to corrugated and planar surfaces are intersecting in nature. Hence, for fixed values of q/k_1 i.e., 0.28 and 0.36; and lower frequencies of wave number, the phase velocity for corrugated surfaces is lower than the phase velocity for planar surfaces. But, this trend gets reversed for higher values of wave number.

Fig. 6(b) represents the favourable effect of q/k_1 on the damping characteristics of torsional waves. However, this effect is not uniform over the entire range of wave number. It is clear from the figure that for both corrugation and corrugation free cases, the effect of q/k_1 on the damped velocity curves is negligible for the region $0 \leq k_1H \leq 1$. Moreover, the damped velocity curves tend to unite in the neighbourhood of k_1H = 6.5 for the case of corrugated boundaries and in the neighbourhood of k_1H = 10.5 for the case of planar boundaries.

6.5 Influence of gravity parameter

To examine the influence of gravity parameter G on the phase and damped velocities of torsional surface waves, the parametric values allotted to G are 0.200, 0.202 and 0.204 for curves 1, 2 and 3, respectively. The graphical analysis has been exhibited through Figs. 7(a) and 7(b).

From Fig. 7(a), it is inferred that the existence of gravity helps the phase velocity of torsional waves to rise up its value for both corrugated and planar bounded surfaces of the layer. Further, the presence of gravity is very much prominent on the phase velocity over the entire region of wave number.

Fig. 7(b) illustrates the fact that the damped velocity curve shifts upwards with the increasing magnitude of gravity parameter. For a fixed value of G, the damped velocity curves corresponding to corrugation and corrugation free cases share a common profile in the region $0 \leq k_1H \leq 4.5$. However, with the rising value of wave number, the damping curves decline rapidly in case of corrugated surfaces than in case of non-corrugated surfaces.

6.6 Influence of position and undulation parameters

Figs. 8(a) and 8(b) illustrate the dynamic response of torsional surface waves under the influence of position (r/H) and undulatory (βH) parameters associated with the corrugated bounded surfaces of the considered layer. In these figures, curves have been plotted for phase (V_P) and damped (V_D) velocities against corrugation parameter ($\gamma\beta$). The numerical values considered for (r/H, βH) are (0.12, 0.12), (0.13, 0.13) and (0.14, 0.14) for curves 1, 2 and 3, respectively.

It is evident from Fig. 8(a) that growing value of (r/H, βH) escalates the phase velocity of torsional waves. However, when the corrugation parameter ($\gamma\beta$) proceeds towards higher values, an opposite trend is followed by the phase velocity curves, i.e., the phase velocity tends to diminish and then finally becomes stable for higher magnitudes of $\gamma\beta$.

Fig. 8(b) elucidates that in the region $0 \leq \gamma\beta \leq 0.36$, the damped velocity curves corresponding to different values of (r/H, βH) are convergent in nature. Hence, it can be concluded that in this region the impact of (r/H, βH) on the damping characteristics is almost negligible. Moreover, the favourable influence of (r/H, βH) on the damped velocity curves is prominently visible for $\gamma\beta > 0.36$.

7. Concluding remarks

In this article, the dispersion and damping attributes of torsional waves in a corrugated Voigt-type viscoelastic porous layer resting over a heterogeneous transversely isotropic gravitating half-space have been examined in detail. The influencing parameters in the presumed geometry are porosity, viscoelasticity, initial stress, heterogeneity and gravity. The impact of these parameters has been exhibited graphically for both corrugated and planar bounded surfaces of the layer. Moreover, graphs have been plotted to irradiate the behavior of phase and damped velocities for increasing magnitudes of corrugation, undulation and position parameters. The remarkable highlights from the current analysis can be encapsulated as:

- The dispersion relation obtained for the isotropic and homogeneous condition is discovered to be in well consent with the pre-established Love wave equation, thus fulfilling the validity of the problem.
- The phase and damped velocities of torsional waves tend to diminish with the growing magnitude of wave number for both corrugated and planar boundary surfaces of the layer.
- The rising value of porosity and viscoelasticity of the layer disfavours the growth of phase and damped velocity curves. Moreover, the effect of these parameters on phase velocity is very much prominent over the entire frequency regime of wave number.
- Initial stress parameters of the layer and half-space exhibit opposite behavior on the phase and damping characteristics of torsional waves. With the increment in the initial stress of the layer, the phase and damped velocity curves shift downwards whereas the phase and damped velocities increase with the growing magnitude of initial stress of the half-space.
- For both corrugation and corrugation free cases, the impact of initial stress of the half-space on the damping curves is negligible in the lower frequencies of wave number. Also, with the presence and growth of initial stress of the half-space, the phase and damped velocities for planar boundaries are always higher than the phase and damped velocities of corrugated boundaries.
- The phase and damped velocities for both corrugated and planar bounded surfaces get boosted with the rise in heterogeneity and gravity parameters associated with the half-space. The influence of these parameters is dominant on the phase velocity curves, whereas the influence is relatively meagre on the damping curves.
- The increment in the position and undulation parameters exhibits a significant as well as positive effect on both the phase and damped velocities of torsional waves. However, the phase and damped velocity curves are independent of the effect of these parameters in the higher and lower frequency regime of corrugation parameter, respectively.

The existence of porosity and viscoelasticity in any corrugated stratified media is an essential characteristic influencing the traversal behavior of seismic waves and assumes an imperative part in numerous geophysical potentialities. Thus, some of the perceptions of the present study may serve as a powerful tool in order to elucidate information in seismic prospecting methods.

Acknowledgements

The authors wish to convey their sincere gratitude to IIT (ISM), Dhanbad, Jharkhand-826004, India, for providing financial support and necessary facilities to Ms. Manisha Maity (IIT(ISM)-JRF) for research work.

References

Abo-Dahab, S.M., Abd-Alla, A.M. and Khan, A. (2016), "Rotational effect on Rayleigh, Love and Stoneley waves in non-homogeneous fibre-reinforced anisotropic general viscoelastic media of higher order", *Struct. Eng. Mech.*, **58**(1), 181–197. https://doi.org/10.12989/sem.2016.58.1.181.

Ahmed, S. M. (1999), "Influence of gravity on the propagation of waves in granular medium", *Appl. Math. Comput.*, **101**(2-3), 269–280. https://doi.org/10.1016/S0096-3003(98)10006-1.

Alam, P., Kundu, S. and Gupta, S. (2017), "Dispersion and attenuation of torsional wave in a viscoelastic layer bonded between a layer and a half-space of dry sandy media", *Appl.Math. Mech.*, **38**(9), 1313-1328. https://doi.org/10.1007/s10483-017-2239-8.

Alam, P., Kundu, S. and Gupta, S. (2018), "Dispersion and Attenuation of Love-Type Waves Due to a Point Source in Magneto-Viscoelastic Layer", *J. Mech.*, **34**(6), 801-816. https://doi.org/10.1017/jmech.2017.110.

Alam, P., Kundu, S. and Gupta, S. (2018), "Dispersion study of SH-wave propagation in an irregular magneto-elastic anisotropic crustal layer over an irregular heterogeneous half-space", *J. King Saud U Sci.*, **30**(3), 301–310. https://doi.org/10.1016/j.jksus.2016.11.007.

Alam, P., Kundu, S. and Gupta, S. (2018), "Effect of magneto-elasticity, hydrostatic stress and gravity on Rayleigh waves in a hydrostatic stressed magneto-elastic crystalline medium over a gravitating half-space with sliding contact", *Mech. Res. Communications*, **89**, 11-17.

https://doi.org/10.1016/j.mechrescom.2018.02.001.
Alam, P., Kundu, S. and Gupta, S. (2018), "Love-type wave propagation in a hydrostatic stressed magneto-elastic transversely isotropic strip over an inhomogeneous substrate caused by a disturbance point source", *J. Intelligent Mater. Syst. Struct.*, **29**(11), 2508-2521. https://doi.org/10.1177/1045389X18770877.
Alam, P., Kundu, S., Gupta, S. and Saha, A. (2018), "Study of torsional wave in a poroelastic medium sandwiched between a layer and a half-space of heterogeneous dry sandy media", *Waves Random Complex Media*, **28**(1), 182-201. https://doi.org/10.1080/17455030.2017.1335915.
Asano, S. (1966), "Reflection and refraction of elastic waves at a corrugated interface", *Bullet. Seismological Soc. America*, **56**(1), 201–221.
Biot, M. A. (1956a), "Theory of deformation of a porous viscoelastic anisotropic solid", *J. Appl. Phys*, **27**(5), 459–467. https://doi.org/10.1063/1.1722402.
Biot, M. A. (1956b), "Theory of elastic waves in a fluid-saturated porous solid: I. Low frequency range", *J. Acoustical Sco. America*, **28**(1), 168–178. https://doi.org/10.1121/1.1908239.
Biot, M. A. (1956c), "Theory of propagation of elastic waves in a fluid-saturated porous solid. II. Higher frequency range", *J. Acoustical Sco. America*, **28**(2), 179–191. https://doi.org/10.1121/1.1908241.
Biot, M. A. (1965), *Mechanics of Incremental Deformations*, John Wiley and Sons, New York.
Carcione, J. M. (1993), "Seismic modeling in viscoelastic media", *Geophysics*, **58**(1), 110–120. https://doi.org/10.1190/1.1443340.
Chattaraj, R. and Samal, S. K. (2013), "Love waves in the fiber-reinforced layer over a gravitating porous half-space", *Acta Geophysica*, **61**(5), 1170–1183. https://doi.org/10.2478/s11600-012-0100-2.
De, S. N. and Sen-Gupta, P. R. (1974), "Influence of gravity on wave propagation in an elastic layer", *J. Acoustical Sco. America*, **55**(5), 919–921. https://doi.org/10.1121/1.1914662.
Elmorabie, K. M. and Yahya, R. R. (2017), "Diffraction of elastic waves from object in layer with slightly corrugated surface", *Math. Mech. Solids*, 1081286517713341.
Gupta, S. and Ahmed, M. (2017), "Influence of pre-stress and periodic corrugated boundary surfaces on Rayleigh waves in an orthotropic medium over a transversely isotropic dissipative semi-infinite substrate", *European Phys J Plus*, **132**(1), 8. https://doi.org/10.1140/epjp/i2017-11282-6.
Gupta, S., Ahmed, M. and Pramanik, A. (2017), "Shear waves in elastic medium with void pores welded between vertically inhomogeneous and anisotropic magnetoelastic semi-infinite media", *Acta Geophysica*, **65**(1), 139–149. https://doi.org/10.1007/s11600-017-0012-2.
Gupta, S., Pati, P., Mandi, A. and Kundu, S. (2018), "Scattering of torsional surface waves in a three-layered model structure", *Struct. Eng. Mech.*, **68**(4), 443-457. https://doi.org/10.12989/sem.2018.68.4.443.
Kakar, R. and Kakar, S. (2016), "Dispersion of shear wave in a pre-stressed heterogeneous orthotropic layer over a pre-stressed anisotropic porous half-space with self-weight", *Struct. Eng. Mech.*, **59**(6), 951–972. https://doi.org/10.12989/sem.2016.59.6.951.
Kumar, R., Singh, K. and Pathania, D.S. (2019), "Shear waves propagation in an initially stressed piezoelectric layer imperfectly bonded over a micropolar elastic half space", *Struct. Eng. Mech.*, **69**(2), 121–129. https://doi.org/10.12989/sem.2019.69.2.121.
Kundu, S., Alam, P., Gupta, S. and Pandit, D. K. (2017), "Impacts on the propagation of SH-waves in a heterogeneous viscoelastic layer sandwiched between an anisotropic porous layer and an initially stressed isotropic half space", *J. Mech.*, **33**(1), 13-22. https://doi.org/10.1017/jmech.2016.43.
Love, A. E. H.(1920), *Mathematical Theory of Elasticity*, Cambridge University Press, Cambridge.
Maity, M., Kundu, S., Pandit, D.K. and Gupta, S. (2018), "Characteristics of torsional wave profiles in a viscous fiber-reinforced layer resting over a sandy half-space under gravity", *J. Geomech.*, **18**(7), https://doi.org/10.1061/(ASCE)GM.1943-5622.0001207.
Ozturk, A. and Akbarov, S. D. (2009), "Torsional wave propagation in a pre-stressed circular cylinder embedded in a pre-stressed elastic medium", *Appl. Math. Model.*, **33**(9), 3636–3649. https://doi.org/10.1016/j.apm.2008.12.003.
Prosser, W. H. and Green Jr, R. E. (1990), "Characterization of the non-linear elastic properties of graphite/epoxy composites using ultrasound", *J. Reinforced Plastics Compos.*, **9**(2), 162–173. https://doi.org/10.1177%2F073168449000900206.
Romenski, E. I., Lys, E. V., Cheverda, V. A. and Epov, M. I. (2014), "Wave propagation in pre-stressed elastic media", *Seismic Technol.*, **11**(4), 1–10.
Selim, M. M. (2007), "Propagation of torsional surface waves in heterogeneous half-space with irregular free surface", *Appl. Math. Sci.*, **1**(29), 1429–1437.
Sharma, M.D. and Gogna, M.L. (1991), "Seismic wave propagation in a viscoelastic porous solid saturated by viscous liquid", *Pure Appl. Geophys.*, **135**(3), 383–400. https://doi.org/10.1007/BF00879471.
Tomar, S. K. and Kaur, J. (2007), "SH-waves at a corrugated interface between a dry sandy half-space and an anisotropic elastic half-space", *Acta Mechanica*, **190**(1-4), 1–28. https://doi.org/10.1007/s00707-006-0423-7.
Vinh, P. C. and Seriani, G. (2010), "Explicit secular equations of Stoneley waves in a non-homogeneous orthotropic elastic medium under the influence of gravity", *Appl. Math. Comput.*, **215**(10), 3515–3525. https://doi.org/10.1016/j.amc.2009.10.047.
Whittaker, E. T. and Watson, G. N. (1991), *A Course of Modern Analysis*, Cambridge University Press, Cambridge.
Winkler, K. and Nur, A. (1979), "Pore fluids and seismic attenuation in rocks", *Geophysical Res. Lett.*, **6**(1), 1–4. https://doi.org/10.1029/GL006i001p00001.

CC

Appendix-I

$$d_1^{'} = \rho_{rr}^{(1)} - \frac{(\rho_{r\theta}^{(1)})^2}{\rho_{\theta\theta}^{(1)}}$$

$$c_1 = \sqrt{\frac{\mu_N}{\rho_1}}$$

$$N_1 = \mu_N + \mathrm{i}\omega\mu_N^{'}$$

$$G_1 = \mu_G + \mathrm{i}\omega\mu_G^{'}$$

$$\xi = \sqrt{\frac{c^2 d_1^{'}}{G_1} - \frac{(N_1 - \frac{P_1}{2})}{G_1}}$$

$G^* = \dfrac{g\rho_2}{\mu_{44}k}$ is the Biot′s gravity parameter

$$c_2 = \sqrt{\frac{\mu_{44}}{\rho_2}}$$

$$\kappa(z) = \frac{G^{*2}k^2}{16\left(1+\frac{P_2}{2\mu_{44}} - \frac{G^* zk}{2}\right)^2} - \frac{q^2}{4} + \frac{G^* kq}{4\left(1+\frac{P_2}{2\mu_{44}} - \frac{G^* zk}{2}\right)} - \frac{k^2\left(\frac{\mu_{11}-\mu_{12}}{2\mu_{44}} - \frac{G^* zk}{2}\right)}{\left(1+\frac{P_2}{2\mu_{44}} - \frac{G^* zk}{2}\right)}\left(1 - \frac{c^2}{c_2^2\left(\frac{\mu_{11}-\mu_{12}}{2\mu_{44}} - \frac{G^* zk}{2}\right)}\right)$$

$$m = \frac{1}{G^*}\left(\frac{c^2}{c_2^2} + \frac{P_2}{2\mu_{44}} - \frac{\mu_{11}-\mu_{12}}{2\mu_{44}} + 1\right) + \frac{q}{4k}$$

$$k_3 = \frac{\sqrt{4k^2+q^2}}{2k}$$

$$a = \frac{4}{G^*}$$

$$b = 1 + \frac{P_2}{2\mu_{44}}$$

$$d = k\frac{G^*}{2}$$

$$J_{11} = k\frac{J_1^{'}(kr)}{J_1(kr)} - \frac{1}{r}$$

$$A_{11} = J_{11}(\mu_N + \mathrm{i}\omega\mu_N^{'})$$

$$A_{22} = k\xi(\mu_G + \mathrm{i}\omega\mu_G^{'})$$

$$\psi_1 = k_3^2 + 4abk_3^3 + 4k_3 m + 4m^2$$

$$\psi_2 = (-8abk_3^3 + 4k_3 m - 4m^2 + k_3^2(3+4q\phi_2(r)))ad^2k_3^2\phi_2(r)$$

$$\psi_3 = d(4a^2b^2k_3^5 - 8m^3 + 2k_3^2 m(-7 + 2abm - 2q\phi_2(r)) - 4k_3 m^2(5+q\phi_2(r)) - k_3^3(3+4abm+q\phi_2(r)) - abk_3^4(3+8q\phi_2(r)))$$

$$a_{11} = \cos(k\xi\phi_2(r))$$

$$a_{12} = \sin(k\xi\phi_2(r))$$

$$a_{13} = -\frac{e^{\frac{k_3 a(b-d\phi_2(r))-q\phi_2(r)}{2}}(-k_3 a(b-d\phi_2(r)))^{-\frac{m}{k_3}}\{1 + \frac{(\frac{m}{k_3}+\frac{1}{2})^2}{k_3 a(b-d\phi_2(r))}\}}{(b-d\phi_2(r))^{\frac{1}{2}}}$$

$$a_{21} = -A_{11}\phi_2^{'}(r)\cos(k\xi\phi_2(r)) - A_{22}\sin(k\xi\phi_2(r))$$

$$a_{22} = A_{22}\cos(k\xi\phi_2(r)) - A_{11}\phi_2^{'}(r)\sin(k\xi\phi_2(r))$$

$$a_{23} = \frac{e^{\frac{k_3 a(b-d\phi_2(r))+q\phi_2(r)}{2}}(-k_3 a(b-d\phi_2(r)))^{-\frac{m}{k_3}}}{8ak_3^4(b-d\phi_2(r))^{\frac{5}{2}}} \{\mu_{44}(bk_3 q\psi_1 + 4a^2d^3k_3^5\phi_2^2(r) + \psi_2 + \psi_3) + J_{11}k_3(\mu_{11}-\mu_{12})(b-d\phi_2(r))(\psi_1 - 4ak_3^3 d\phi_2(r))\phi_2^{'}(r)\}$$

$$a_{31} = -A_{11}\phi_1^{'}(r)\cos(k\xi(\phi_1(r)-H)) - A_{22}\sin(k\xi(\phi_1(r)-H))$$

$$a_{32} = A_{22}\cos(k\xi(\phi_1(r)-H)) - A_{11}\phi_1^{'}(r)\sin(k\xi(\phi_1(r)-H))$$

Appendix-II

$$\chi_1 = -(A_{22}(4a^2d^3e^{q\phi_2(r)}k_3^5\mu_{44}\phi_2^2(r) + 2A_{11}k_3(k_3+2m)^2 (b-d\phi_2(r))(\phi_1^{'}(r)-\phi_2^{'}(r)) + 4ak_3^4(b-d\phi_2(r)) (2A_{11}(b-d\phi_2(r))(\phi_1^{'}(r)-\phi_2^{'}(r)) - de^{q\phi_2(r)}J_{11}(\mu_{11}-\mu_{12})\phi_2(r)\phi_2^{'}(r)) + e^{q\phi_2(r)}(-dJ_{11}k_3(\mu_{11}-\mu_{12})\phi_2(r)\phi_2^{'}(r)\psi_1 + bk_3(q\mu_{44} + J_{11}(\mu_{11}-\mu_{12})\phi_2^{'}(r))\psi_1 + \mu_{44}(\psi_2+\psi_3))))$$

$$\chi_2 = (-2k_3(b-d\phi_2(r))(k_3^2 + 4k_3 m + 4m^2 + 4ak_3^3(b-d\phi_2(r))) (A_{22}^2 + A_{11}^2\phi_1^{'}(r)\phi_2^{'}(r)) + A_{11}e^{q\phi_2(r)}\phi_1^{'}(r)(4a^2d^3k_3^5\mu_{44}\phi_2^2(r) - 4adJ_{11}k_3^4(\mu_{11}-\mu_{12})\phi_2(r)(b-d\phi_2(r))\phi_2^{'}(r) - dJ_{11}k_3(\mu_{11}-\mu_{12})\phi_2(r)\phi_2^{'}(r)\psi_1 + bk_3(q\mu_{44} + J_{11}(\mu_{11}-\mu_{12})\phi_2^{'}(r))\psi_1 + \mu_{44}(\psi_2+\psi_3)))$$

$$\psi_{22} = (-8abk_3^3 + 4k_3 m - 4m^2 + k_3^2(3+4q\gamma_2\cos(\beta r))) ad^2k_3^2\gamma_2\cos(\beta r)$$

$$\psi_{33} = d(4a^2b^2k_3^5 - 8m^3 + 2k_3^2m(-7 + 2abm - 2q\gamma_2\cos(\beta r)) - 4k_3m^2(5 + q\gamma_2\cos(\beta r)) - k_3^3(3 + 4abm + q\gamma_2\cos(\beta r)) - abk_3^4(3 + 8q\gamma_2\cos(\beta r)))$$

$$\chi_{11} = -(A_{22}(4a^2d^3e^{q\gamma_2\cos(\beta r)}k_3^5\mu_{44}\gamma_2^2\cos^2(\beta r) + 2A_{11}k_3(k_3 + 2m)^2(b - d\gamma_2\cos(\beta r)) \gamma_2\beta\sin(\beta r) - \gamma_1\beta\sin(\beta r)) + 4ak_3^4(b - d\gamma_2\cos(\beta r)) (2A_{11}(b - d\gamma_2\cos(\beta r))(\gamma_2\beta\sin(\beta r) - \gamma_1\beta\sin(\beta r)) + de^{q\gamma_2\cos(\beta r)}J_{11}(\mu_{11} - \mu_{12})\gamma_2^2\beta\cos(\beta r)\sin(\beta r)) + e^{q\gamma_2\cos(\beta r)}(dJ_{11}k_3(\mu_{11} - \mu_{12})\gamma_2^2\beta\cos(\beta r)\sin(\beta r)\psi_1 + bk_3(q\mu_{44} - J_{11}(\mu_{11} - \mu_{12})\gamma_2\beta\sin(\beta r))\psi_1 + \mu_{44}(\psi_{22} + \psi_{33}))))$$

$$\chi_{22} = (-2k_3(b - d\gamma_2\cos(\beta r))(k_3^2 + 4k_3m + 4m^2 + 4ak_3^3(b - d\gamma_2\cos(\beta r)))(A_{22}^2 + A_{11}^2\gamma_1\gamma_2\beta^2\sin^2(\beta r)) - A_{11}e^{q\gamma_2\cos(\beta r)}\gamma_1\beta\sin(\beta r)(4a^2d^3k_3^5\mu_{44}\gamma_2^2\cos^2(\beta r) + 4adJ_{11}k_3^4(\mu_{11} - \mu_{12})(b - d\gamma_2\cos(\beta r))\gamma_2^2\beta\sin(\beta r)\cos(\beta r) + dJ_{11}k_3(\mu_{11} - \mu_{12})\gamma_2^2\beta\sin(\beta r)\cos(\beta r)\psi_1 + bk_3(q\mu_{44} - J_{11}(\mu_{11} - \mu_{12})\gamma_2\beta\sin(\beta r))\psi_1 + \mu_{44}(\psi_{22} + \psi_{33})))$$

$$\psi_{333} = d(4a^2b^2k_3^5 - 8m^3 + 2k_3^2m(-7 + 2abm) - 20k_3m^2 - k_3^3(3 + 4abm) - 3abk_3^4)$$

$$c_{11} = \sqrt{\frac{\mu_1}{\rho_1}}$$